# Temporal upscaling of instantaneous evapotranspiration on clear-sky days using the constant reference evaporative fraction method with fixed or variable surface resistances at two cropland sites

Ronglin Tang, Zhao-Liang Li, Xiaomin Sun, Yuyun Bi

# Temporal upscaling of instantaneous evapotranspiration on clear-sky days using the constant reference evaporative fraction method with fixed or variable surface resistances at two cropland sites

**Ronglin Tang[1], Zhao-Liang Li[2,3,*], Xiaomin Sun[4] and Yuyun Bi[2]**

[1]State Key Laboratory of Resources and Environment Information System, Institute of Geographic Sciences and Natural Resources Research, Beijing 100101, China.

[2]Key Laboratory of Agri-informatics, Ministry of Agriculture/Institute of Agricultural Resources and Regional Planning, Chinese Academy of Agricultural Sciences, Beijing 100081, China.

[3]ICube, UdS, CNRS; 300 Bld Sebastien Brant, CS10413, 67412 Illkirch, France.

[4]Key Laboratory of Ecosystem Network Observation and Modeling, Institute of Geographic Sciences and Natural Resources Research, Beijing 100101, China.

Corresponding author: Zhao-Liang Li (lizhaoliang@caas.cn)

**Key Points:**

- The constant reference evaporative fraction upscaling method was tested.
- Fixed and variable surface resistances were compared in the ET upscaling.
- Analysis was made over different assumed satellite overpass times.

## Abstract

Surface evapotranspiration (ET) is an important component of water and energy in land and atmospheric systems. This paper investigated whether using variable surface resistances in the reference ET estimates from the full-form Penman-Monteith (PM) equation could improve the upscaled daily ET estimates in the constant reference evaporative fraction ($EF_r$, the ratio of actual to reference grass/alfalfa ET) method on clear-sky days using ground-based measurements. Half-hourly near-surface meteorological variables and eddy covariance (EC) system-measured latent heat flux data on clear-sky days were collected at two sites with different climatic conditions, namely, the sub-humid Yucheng station in northern China and the arid Yingke site in northwestern China and were used as the model input and ground-truth, respectively. The results showed that using the FAO-PM equation, the ASCE-PM equation, and the full-form PM equation to estimate the reference ET in the constant $EF_r$ method produced progressively smaller upscaled daily ET at a given time from mid-morning to mid-afternoon. Using all three PM equations produced the best results at noon at both sites regardless of whether the energy imbalance of the EC measurements was closed. When the EC measurements were not corrected for energy imbalance, using variable surface resistance in the full-form PM equation could improve the ET upscaling in the mid-afternoon, but worse results may occur in the mid-morning to noon. Site-to-site and time-to-time variations were found in the performances of a given PM equation (with fixed or variable surface resistances) before and after the energy imbalance was closed.

**Key words:** evapotranspiration; reference evaporative fraction method; temporal upscaling; fixed or variable resistance

## 1 Introduction

Land surface evapotranspiration (ET, water in mm equivalent to latent heat flux) is one of the most significant components of the global hydrological cycle, and its estimation plays a significant role in numerical weather forecasting, global climate change modeling, and irrigation water allocation. Although many eddy covariance sites have been established worldwide in the past several decades to measure the long-term transfer of surface water, heat, and momentum across different ecosystems [*Baldocchi et al.,* 2001], these measurements are spatially discrete and of limited spatial representativeness. Remote sensing technology provides the ability to map surface ET over large heterogeneous areas and complements conventional ground-based ET measurements at the tower scale. Because remote sensing models of ET estimation can generally only provide instantaneous values at the clear-sky satellite overpass time [*Kalma et al.*, 2008; *Li et al.,* 2009; *Tang et al.,* 2010, 2012], several upscaling methods have been developed to convert instantaneous ET data to a daily value so that water consumption by crops can be monitored [*Shuttleworth et al.,* 1989; *Trezza,* 2002; *Jackson et al.*, 1983; *Brutsaert and Sugita,* 1992; *Ryu et al.,* 2012; *Van Niel et al.*, 2012; *Delogu et al.,* 2012].

The constant reference evaporative fraction [$EF_r$, the ratio of actual to reference grass (alfalfa) ET] method, which was proposed by *Trezza* [2002] to use a fixed surface resistance of 50 (30) s/m during the daytime and 200 s/m during the nighttime for reference grass (alfalfa) ET estimates and assumes that $EF_r$ is relatively constant during the day, is one of the most widely applied schemes for upscaling instantaneous remote sensing estimates of ET. The effectiveness of the constant $EF_r$ method in upscaling instantaneous ET data has been investigated and demonstrated by numerous studies that used primarily local (in-situ) metrological observations

[*Colaizzi et al.*, 2006; *Chávez et al.*, 2008; *Allen et al.*, 2007; *Liu et al.*, 2012; *Tang et al.*, 2013a]. Biases may be found when this method is tested using only remote sensing data [*Cammalleri et al.*, 2014].

The key to using the constant $EF_r$ method is to accurately estimate the instantaneous (or half-hourly/hourly) and daily ET values for a reference crop using the Penman-Monteith (PM) equation. A fixed surface resistance of 70 s/m was adopted by FAO56 for the reference grass ET estimate from the PM (hereafter referred to as FAO-PM) equation for hourly and daily time steps [*Allen et al.*, 1998]. By comparing the major reference ET equations using weather data from diverse climates across the United States, the Environmental and Water Resources Institute of the American Society of Civil Engineers [*ASCE-EWRI*, 2005] recommended using a fixed surface resistance of 50 s/m during the daytime and 200 s/m during the nighttime for shorter reference grass ET estimates from the PM (hereafter referred to as ASCE-PM) equation at hourly or shorter computation steps.

Surface resistance not only is a physiological parameter but also has an aerodynamic component. The surface resistance over the course of a day is essentially time-dependent and can be influenced by variations in solar radiation, vapor pressure deficit, and wind speed even for the water-unstressed reference grass/alfalfa surface. *Katerji and Perrier* [1983] related the surface resistance to aerodynamic resistance and climatological variables through a linear model. However, the coefficients in their model must be experimentally calibrated before they can be applied to grass and alfalfa. *Alves and Pereira* [2000] reported that the model can be applied only under a limited range of Bowen ratio conditions. *Todorovic* [1999] also modeled the surface resistance as a function of aerodynamic resistance and climatic variables, but his model does not require a priori calibration and can be applied without additional constraints. Both surface resistance models have been widely used in the application of the PM equation, and several authors have recommended them for practical use because they provide better estimates of the reference ET than using a fixed value of 70 s/m [*Pereira et al.*, 1999; *Rana and Kaerji*, 2000; *Lecina et al.*, 2003; *Perez et al.*, 2006; *Liu et al.*, 2012].

To the best of our knowledge, almost all recent investigations of the constant $EF_r$ upscaling method have used a fixed surface resistance of 50 s/m during the daytime periods to estimate the reference short grass (or 30 s/m for the reference tall alfalfa) ET as recommended by the ASCE-EWRI [*Colaizzi et al.*, 2006; *Allen et al.*, 2007; *Chávez et al.*, 2008; *Tang et al.*, 2013a]. No studies have ever attempted to incorporate a variable daytime surface resistance in the upscaling of instantaneous ET data using the constant $EF_r$ method. Similar upscaled daily ET results can be expected to be obtained when the daytime variable surface resistance is close to the fixed values of 70 s/m in the FAO-PM equation or 50 s/m in the ASCE-PM equation. Additional studies are necessary to assess the performance of the constant $EF_r$ upscaling method under extreme climatic conditions, when the variable surface resistance significantly deviates from the commonly used fixed value.

The objective of this study is to use ground-based measurements to investigate whether using a variable surface resistance in the reference ET estimate from the PM equation can improve the daily (24-h) upscaled ET result of the constant $EF_r$ method. Section 2 describes the derivation of the variable surface resistance, the formulations of the three reference ET estimation methods, and the ET-upscaling theory. Section 3 presents the validation sites, the procedures for selecting clear days during each of the three daytime periods, and the method of correcting the energy imbalance in the EC-measured fluxes. In section 4, the daily ETs that are

upscaled using the three reference ET estimation methods are compared and validated. A summary and conclusions are provided in Section 5.

## 2 Methodology

### 2.1 Derivation of variable surface resistance

Based on the principle of surface energy balance, the difference between the potential ET and actual ET (reference ET in this paper) can be assumed to be caused by an additional sensible heat flux imposed to heat the vegetation surface to provide the extra energy to move saturated air out of vegetation elements. *Todorovic* [1999] predicted this additional sensible heat flux as a function of a ‘‘pseudo’’ resistance to the additional sensible heat transfer and the difference between the temperature on the potential ET surface and that on the actual ET surface. With the assumption that the ‘‘pseudo’’ resistance equals the surface resistance and the temperature difference is approximated as a function of the vapor pressure deficit and air temperature, the surface resistance can be estimated by combining the ET estimated from the PM equation and the additional sensible heat into the surface energy balance equation. A detailed description of the theory and development of the model can be found in *Todorovic* [1999]. Here, we focus on the formulations that are used to obtain the surface resistance. In Todorovic's method, the variable surface resistance during the daytime can be solved through the following quadratic equation:

$$a\left(\frac{r_s}{r_c}\right)^2 + b\frac{r_s}{r_c} + c = 0 \tag{1}$$

where $r_s$ is the surface resistance, s/m; and $r_c$ is the climatological resistance, s/m. The coefficients *a*, *b*, and *c* and the climatological resistance can be derived as follows:

$$r_c = \rho c_p \frac{e_s - e_a}{\gamma \times E} \tag{2}$$

$$a = \frac{\Delta + \gamma(r_c / r_a)}{\Delta + \gamma}(r_c / r_a)(e_s - e_a) \tag{3}$$

$$b = -\gamma \frac{e_s - e_a}{\Delta + \gamma}\frac{r_c}{r_a}\frac{\gamma}{\Delta} \tag{4}$$

$$c = -(\Delta + \gamma)\frac{e_s - e_a}{\Delta + \gamma}\frac{\gamma}{\Delta}, \tag{5}$$

where $\Delta$ is the slope of the saturated vapor pressure versus the air temperature curve, kPa/°C; ρ is the air density, kg/m$^3$; $c_p$ is the specific heat of the air, J/(kg·°C); $e_s$-$e_a$ is the vapor pressure deficit of the air, kPa; γ is the psychrometric constant, kPa/°C; *E* is the surface available energy and equals surface net radiation minus soil heat flux, W/m$^2$; and $r_a$ is the aerodynamic resistance, s/m. Eq. (1) has only one positive surface resistance solution.

## 2.2 Estimation of Reference ET

### 2.2.1 Full-form PM equation

Using the solved variable surface resistance from Eq. (1) at the hourly (or half-hourly) time scale, the reference ET during the daytime can be derived from the "full-form" PM combination equation:

$$ET_{TOD-PM} = \frac{\Delta(R_n - G) + \rho c_p (e_s - e_a)/r_a}{\Delta + \gamma(1 + r_s / r_a)} \tag{6}$$

where $R_n$ is the surface net radiation; $G$ is the soil heat flux; $ET_{TOD-PM}$ is the reference ET estimated using the variable surface resistance that is derived from Todorovic's method.

A short reference crop and a tall reference crop, as proposed by *ASCE-EWRI* [2005], are adopted to estimate the reference ET for wheat and corn, respectively. When the full-form PM equation is applied to the reference short/tall crop, this equation can be reduced to a simplified form given that $r_a$ can be estimated with the procedure presented by *Allen et al.* [1998]. The simplified PM equation can be expressed as

$$ET_{TOD-PM} = \frac{0.408\Delta(R_n - G) + \gamma \frac{C_n}{T_a + 273} u_2 (e_s - e_a)}{\Delta + \gamma(1 + C_d u_2)}, \tag{7}$$

$$C_d u_2 = r_s / r_a = \begin{cases} \frac{u_2}{208} r_s & \textit{short grass} \\ \frac{u_2}{118} r_s & \textit{tall alfalfa} \end{cases}, \tag{8}$$

where $R_n$ and $G$ are expressed in units of MJ/(m$^2$·d); $u_2$ is the wind speed measured at 2 m height, m/s; $T_a$ is the air temperature, °C; and $C_n$ and $C_d$ are the coefficients that change with surface resistance. For the reference short grass, $C_n$ equals 900 at the daily scale and 37 at the hourly scale. For the reference tall alfalfa, $C_n$ equals 1600 at the daily scale and 66 at the hourly scale. From Eq. (8), $r_a$ equals $208/u_2$ for short grass and $118/u_2$ for tall alfalfa. During the nighttime period, the surface resistance is fixed at 200 s/m for both reference surfaces, as is done in the ASCE-PM equation (see Section 2.2.3). With the exception of the surface resistance, the calculation of each of the variables in Eq. (7) closely follows the procedures specified by *ASCE-EWRI* [2005].

### 2.2.2 FAO-PM equation

In the standard FAO-PM equation [*Allen et al.*, 1998], the reference ET is estimated with the simplified PM equation for a hypothetical grass (or alfalfa) with an assumed height of 0.12 m (or 0.5 m), a fixed surface resistance of 70 (or 45) s/m, and an albedo of 0.23 for both the daily and hourly time steps. The FAO-PM equation has the same formulation as Eq. (7). The only difference is that the coefficient $C_d$ equals 0.34 for the reference short grass and 0.38 for the reference tall alfalfa for a daily cycle in the FAO-PM equation.

### 2.2.3 ASCE-PM equation

In the standard ASCE-PM equation [*ASCE-EWRI*, 2005] for the reference short grass (tall alfalfa), the fixed resistance of 70 (45) s/m used in the FAO-PM equation is replaced by a lower value of 50 (30) s/m during the daytime and a higher value of 200 s/m during the nighttime. The ASCE-PM equation also has the same formulation as Eq. (7). The only difference is that the coefficient $C_d$ equals 0.24 (0.25) during daytime and 0.96 (1.7) during nighttime for the reference short grass (tall alfalfa) in the ASCE-PM equation.

## 2.3. Upscaling of instantaneous ET

After the half-hourly or hourly reference ET value is estimated with the three PM equations, assuming that the ratio of the actual instantaneous ET to daily ET values equals the ratio of the corresponding reference instantaneous ET to daily ET values, the actual daily ET can be derived as follows:

$$ET_{a,d} = \frac{ET_{r,d}}{ET_{r,i}} ET_{a,i} \tag{9}$$

where $ET_{r,i}$ and $ET_{a,i}$ are the reference ET value and the actual ET value at the instantaneous time scale, respectively; $ET_{r,d}$ and $ET_{a,d}$ are the reference ET value and the actual ET value at the daily (24-h) time scale, respectively. The $ET_{r,i}$ can be estimated from the full-form PM equation, the FAO-PM equation, or the ASCE-PM equation; the $ET_{r,d}$ is estimated by summing the half-hourly $ET_{r,i}$ values over a diurnal cycle. The $ET_{a,i}$ comes from the half-hourly ground-based eddy covariance measurements that are uncorrected for energy imbalance or corrected by the Bowen ratio and the residual energy methods (see Section 3.3).

# 3 Test site and data

## 3.1 Test site

Data were collected at two sites (Yucheng and Yingke; see Table 1), which are characterized by contrasting climatic conditions in China, to investigate the use of the constant $EF_r$ method to upscale instantaneous ET data. The Yucheng site is located in the North China Plain and has a sub-humid monsoon climate and a sandy loam soil texture. Winter wheat (October to June) and summer corn (June to October) are rotated each year. Approximately 60-70% of the annual rainfall occurs during the summer corn growing season, and the remaining 30-40% falls during the winter wheat growing season. The Yingke site is located in an irrigated field in the middle reaches of the Heihe River Basin in northwestern China and is characterized by an arid climate and a silt loam soil texture. Corn is interplanted with spring wheat from May to July and the site is covered by corn only from August to September.

Both sites are equipped with standard sensors (Table 2) that measure meteorological variables (e.g., air temperature, air pressure, actual vapor pressure, and wind speed/direction) and the soil water and temperature profiles at 30-min intervals. Downward and upward shortwave and longwave radiation are measured with a CNR-1 device at both sites, and the soil heat flux ($G$) is measured with an HFP-01 soil heat flux plate at a depth of 2 cm at the Yucheng site and 5 cm at the Yingke site. Heat storage above the plate is not accounted for because no more information is available at hand for its correction. Over the entire study period, the multi-day mean surface available energy ($R_n$-$G$) at the Yingke site is much larger than that at the Yucheng

site; the difference can be as much as ~100 W/m$^2$ at noon (see Figure 1a). In contrast, the multi-day mean wind speed ($u$) at the Yingke site is ~1.3 m/s lower than that at the Yucheng site (Figure 1b). Moreover, the maximum wind speed at the Yucheng site generally occurs at noon, whereas the maximum wind at the Yingke site occurs in the mid-afternoon. The daytime wind speed at the Yingke site is more asymmetric than that at the Yucheng site. The multi-day mean vapor pressure deficit (*VPD*) at the Yingke site is slightly higher than that at the Yucheng site and has a maximum value of ~1.5 kPa. Over the involved clear-sky days (see Section 3.2 for the selection rules) that are selected for the model assessment, the multi-day mean surface available energy is slightly and moderately (difference < 70 W/m$^2$) larger at the Yingke site and Yucheng site, respectively, than that over the entire study period from mid-morning to mid-afternoon. The multi-day mean surface available energy at the Yingke site is still larger than that at the Yucheng site, but their difference (< 50 W/m$^2$) becomes smaller than that over the entire study period. The multi-day mean wind speed at the Yucheng and Yingke sites over the selected clear-sky days is moderately higher than (difference < 0.6 m/s) and has a similar magnitude to that over the entire study period, respectively, which causes a much larger difference (as high as 1.8 m/s) in wind speed between the Yucheng site and the Yingke site over the selected clear-sky days. Both the Yucheng and the Yingke sites have slightly larger multi-day mean *VPD* over the selected clear-sky days than over the entire study period from the mid-morning to mid-afternoon. A negligible difference is observed in the multi-day mean *VPD* between the Yucheng and the Yingke sites over the selected clear-sky days.

**Table 1.** Attributes of the two sites in China used for the evaluation of the constant reference evaporative fraction upscaling method (AP: Annual mean precipitation, mm; AT: Annual mean temperature, ºC)

| Site | Longitude (E) | Latitude (N) | Land cover | Elevation(m) | AP | AT | Data period |
|---|---|---|---|---|---|---|---|
| Yucheng | 116.5703 | 36.8291 | Crop | 28 | 582 | 13.1 | 04/2009-06/2012 |
| Yingke | 100.4103 | 38.8571 | Crop | 1519 | 127 | 7.2 | 01/2008-11/2009 |

**Table 2.** Description of the model, manufacturer, and location for the instruments/sensors at the Yucheng [*Yu et al.*, 2007; *Sun et al.*, 2009] and the Yingke [*Liu et al.*, 2011] sites involved in this study. $T_a$ and $e_a$: air temperature and actual vapor pressure; $u$: wind speed; *WD*: wind direction; $R_s$: shortwave radiation; $R_l$: longwave radiation; $G$: soil heat flux; *Pa*: atmospheric pressure; $T_s$: soil temperature; *SM*: soil moisture; H and LE: sensible and latent heat fluxes.

| Site | $T_a$ and $e_a$ | $u$ | *WD* | $R_s$ | $R_l$ | $G$ | *Pa* | $T_s$ | *SM* | H and LE |
|---|---|---|---|---|---|---|---|---|---|---|
| Yucheng | HMP45C, Vaisala, Helsinki, Finland | A100R, Vector Instruments, Rhyl, UK | W200P, Vector Instruments, Rhyl, UK | CNR-1, Kipp & Zonen, Delft, Netherlands | CNR-1, Kipp & Zonen, Delft, Netherlands | HFP01, HUKSEFLUX, Delft, Netherlands | CS105, VAISALA, Helsinki, Finland | STP01, HUKSEFLUX, Delft, Netherlands | CS616, Campbell Scientific, Utah, USA | CSAT3/LI-7500, Campbell Scientific /Li-Cor, Utah/ Nebraska, USA |
| Yingke | | 010C-1, Metone Instruments, Oregon, USA | 020C-1, Metone Instruments, Oregon, USA | CM3, Kipp & Zonen, New York, USA | CG3, Kipp & Zonen, New York, USA | HFP01, Campbell Scientific, Utah, USA | CS100, Campbell Scientific, Utah, USA | 109, Campbell Scientific, Utah, USA | | |

**Table 3.** Number of the clear-sky and partly cloudy days that had clear skies at three different daytime periods from April 2009 to June 2012 at the Yucheng site and from January 2008 to November 2009 at the Yingke site.

| Site | Time period | | |
|---|---|---|---|
| | 10:00-11:00 | 12:00-13:00 | 14:00-15:00 |
| Yucheng | 77 | 68 | 100 |
| Yingke | 76 | 73 | 80 |

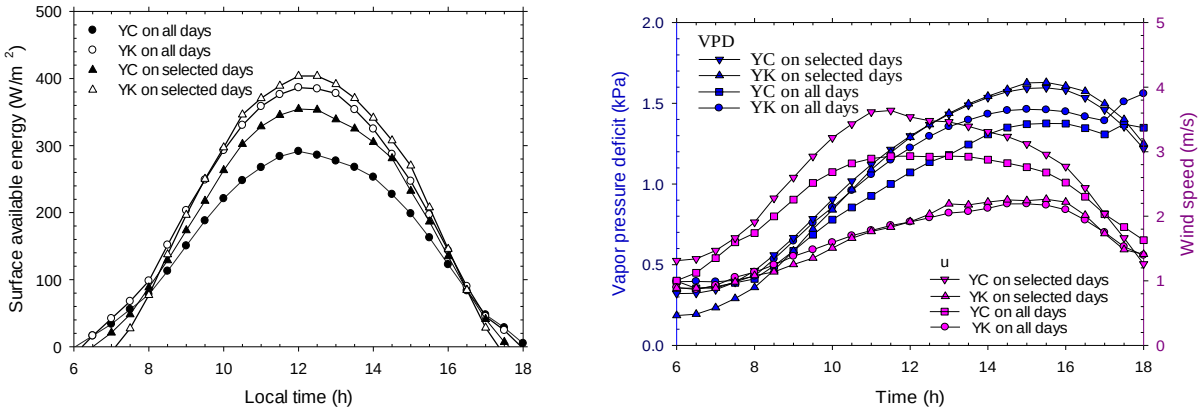


**Figure 1**. Daytime variations of ground-based measurements of (**a**) surface available energy ($R_n$-$G$), (**b**) vapor pressure deficit (*VPD*) and wind speed ($u$), averaged from April 1, 2009 to June 30, 2012 or over the selected 125 clear-sky days at the Yucheng (YC) site and from January 1, 2008 to November 30, 2009 or over the selected 93 clear-sky days at the Yingke (YK) site.

The thirty-minute averaged sensible heat flux (H) and latent heat flux (LE) are regularly measured by an eddy covariance (EC) system that consists of an open-path $CO_2$/$H_2O$ gas analyzer (model LI-7500, Licor Inc., Lincoln, Nebraska) and a 3-D sonic anemometer/thermometer (model CSAT3, Campbell Scientific Inc., Logan, Utah) at both sites. The EC sensor is elevated to ~4.3 m above surface level (ASL) in late July or early August and is lowered to ~2.9 m ASL in mid- to late-October every year at the Yucheng site but is fixed at ~2.8 m ASL at the Yingke site. At the Yucheng and Yingke sites, the relative height of the EC sensor is ~2.1 m and ~1.8 m above maximum wheat height and ~1.7 m and ~1.0 m above the maximum corn height, respectively. The main contributing area of the EC measurements is within 180 m and 100 m around the sensor at the Yingke and Yucheng sites [*Liu et al.*, 2011; *Tang et al.*, 2011a], respectively. To obtain reliable EC-measured H and LE data using the online flux computation and post-field data programs [*Yu et al.*, 2006; *Liu et al.*, 2011], a series of corrections are performed on the effect of the sonic virtual temperature, the time-lag, the performance of the planar fit coordinate rotation, the density fluctuation, and the frequency response following *Webb et al.* [1980] and *Burba and Anderson* [2010].

Half-hourly averaged atmospheric variables (global solar radiation, air temperature, wind speed, relative humidity, and atmospheric pressure) were collected from April 2009 to June 2012 at the Yucheng site and from January 2008 to November 2009 at the Yingke site. The data were used to drive the reference ET model and the daily (24-h) averaged latent heat flux measured by the EC with and without an energy imbalance correction to validate the upscaled value from the constant $EF_r$ method. These data were carefully checked to ensure the quality and completeness of the daily cycle in two steps. First, data spikes and abnormalities in the measured H and LE (less than -100 W/m$^2$ or greater than 700 W/m$^2$ [*Tang et al.*, 2013; *Liu et al.*, 2011], which approximate the lower and upper limits of surface net radiation) were removed, and then days with data gaps caused by rainfall events, instrument malfunctions or maintenance, and data spikes and abnormalities in the 30-min averaged atmospheric variables or EC-measured H and LE were excluded. After these data quality and completeness checks, 485 days from April 2009 to June 2012 at the Yucheng site and 272 days from January 2008 to November 2009 at the Yingke site were available for further analysis. The daily measured surface fluxes (surface net

radiation, soil heat flux, sensible heat flux, and latent heat flux) can be obtained by averaging the 48 half-hourly measurements of each diurnal cycle.

### 3.2 Selection of days with a clear sky at the assumed "satellite overpass" time

To recognize the possible time dependencies of the uncertainties and errors, the instantaneous ET values from three daytime periods (10:00-11:00, 12:00-13:00, and 14:00-15:00 local time) between mid-morning and mid-afternoon, which correspond to the overpass times of most of the polar-orbiting satellites, were upscaled. The upscaling of the instantaneous ET data is generally restricted to clear-sky satellite overpass times in practical applications [*Li et al.*, 2013a, 2013b]. The evaluation at both sites therefore focuses on days that have clear skies at the assumed satellite overpass times. Because the climatological resistance in the denominator on the left-hand side of Eq. (1) cannot equal zero, the relative humidity of the atmosphere during the daytime period for a given selected clear or partly cloudy day should be less than 100%, as seen in Eq. (2), which leads to a reduction in the available days to 355 days at the Yucheng site and 208 days at the Yingke site. Though some authors have suggested estimating potential surface solar radiation as a factor of extraterrestrial radiation [e.g., *Allen et al.* [1998] assigned this factor to be 0.75 at sea level and incorporated the elevation to this factor above this level], the ratio of the observed clear-sky solar radiation to extraterrestrial radiation in previous studies [*Todorovic et al.*, 1999] and at the two sites in this study is shown to vary diurnally and seasonally. Determining whether a day is clear by comparing the observed surface solar radiation to the potential surface solar radiation determined as a fixed factor of extraterrestrial radiation is likely to miss some days. Here, we briefly review the two-step procedure that was proposed by *Tang et al.* [2013a] to identify the days that have clear skies at the different time intervals.

First, days that are clear during the entire daytime period are selected by analyzing the observed half-hourly global solar radiation and the corresponding shortwave atmospheric transmissivity ($\tau$, the ratio of the observed global solar radiation to the extraterrestrial solar radiation). If both values on a given day increase monotonically from sunrise (global solar radiation > 5 W/m$^2$) to midday and then decrease monotonically from midday to sunset (global solar radiation > 5 W/m$^2$), then that day will be classified as a clear-sky day and will be used for further analysis. Moreover, a visual check is made of the selected clear-sky days to remove those that are covered by constant cloud cover during the daytime.

Next, days that are partly cloudy during the daytime but have clear skies at the assumed satellite overpass times are selected. Days that do not have clear skies or constant cloud cover over the entire daytime period are classified as partly cloudy days. For each of the three different daytime periods, if the vertical-path shortwave atmospheric transmissivity ( $\tau_0 = \tau^{\cos\theta}$, where $\tau$ is the slant-path transmissivity at the solar zenith angle $\theta$) on a given partly cloudy day is greater than the minimum of the corresponding $\tau_0$ from two adjacent clear days, then that partly cloudy day will be selected for further analysis.

With the constraints provided by these selection criteria, 77 (76) clear-sky and partly cloudy days had clear skies at 10:00-11:00, 68 (73) days were clear at 12:00-13:00, and 100 (80) days were clear at 14:00-15:00 at the Yucheng (Yingke) site (see Table 3). The half-hourly meteorological variables and turbulent heat fluxes on these days were used to evaluate and validate the constant $EF_r$ method.

### 3.3 Correction of the energy imbalance in the EC measurements

The energy imbalance in surface EC measurements has been reported in numerous studies [*Twine et al.*, 2000; *Wilson et al.*, 2002; *Foken*, 2008; *Tang et al.*, 2011b, 2013b; *Stoy et al.*, 2013]. In most cases, the sum of the measured H and LE is less than the measured surface available energy. Although no consensus has been reached on how to best reconcile this energy imbalance, the Bowen ratio (BR) correction method and the residual energy (RE) correction method, which were proposed by *Twine et al.* [2000] and have been widely applied in previous years, are adopted in this study to correct the daytime 30-min averaged EC measurements to evaluate the $EF_r$ upscaling method under energy-closure conditions. In the BR correction method, the surface available energy is repartitioned into H and LE by conserving the original EC-measured Bowen ratio. In the RE correction method, all of the imbalanced energy goes into the measured LE. When the RE correction method is directly applied to each of the corresponding 30-min averaged LE measurements in a diurnal cycle, the daily LE after correction averaged over the clear-sky or partly cloudy days is shown to be less than that before correction due to the negative available energy during the nighttime, which seems unreliable and is primarily caused by the limitation of the correction method during the nighttime. Moreover, the BR correction method is found to be corrupted if the sum of the original H and LE is close to zero during the nighttime. Therefore, we assume that the ratio of the EC-measured daytime to daily LE before and after the correction is constant to derive the corrected daily LE measurement after applying the BR and RE correction methods to the daytime 30-min averaged EC measurements.

## 4 Results and discussion

### 4.1 Daytime variation in Todorovic's surface resistance and the noon-time evolution of the flux ratio

Before evaluating the performance of the constant $EF_r$ method in upscaling instantaneous ET, the daytime variation in the half-hourly surface resistance estimated by Todorovic's method is examined in Figure 2. These daytime surface resistances were averaged over the days that had clear skies at 12:00-13:00 local time for the wheat and corn growth stages at the Yucheng and Yingke sites. Figure 2 clearly shows that the daytime surface resistance estimated from Eq. (1) exhibits a concave shape with the minimum occurring at noon and the maximum in the early morning or late afternoon. The averaged daytime surface resistance for the wheat (short crop) growth period was higher than that for the corn (tall crop) growth period at both sites. For both the wheat and corn growth periods, the estimated daytime surface resistance at the Yucheng site was between the fixed values recommended by the FAO-PM (70 s/m for short grass and 45 s/m for tall alfalfa) and the ASCE-PM (50 s/m for short grass and 30 s/m for tall alfalfa) equations near noon time (10:00 h - 14:00 h) but was higher than them in the early morning and late afternoon. At the Yingke site, the variable surface resistance was higher than the fixed values recommended by the FAO-PM and the ASCE-PM equations.

The concave shape and site-to-site differences in the surface resistance are primarily determined by the daytime evolution of the meteorological variables of surface available energy, vapor pressure deficit, and wind speed at both sites; the sensitivity analysis presented in Figure 3 shows that a high vapor pressure deficit, a low wind speed, a low surface available energy, and a low air temperature can all lead to a high surface resistance and vice versa. Moreover, the sensitivity of the surface resistance to the surface available energy (wind speed, air temperature)

decreases when the surface available energy (wind speed, air temperature) increases, and a higher sensitivity can be obtained with a higher vapor pressure deficit.

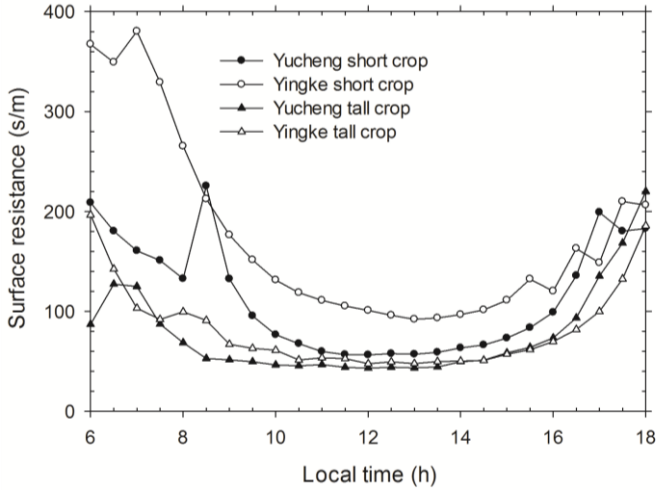


**Figure** 2. Daytime variations of half-hourly surface resistances estimated from the method proposed by *Todorovic* [1999] and averaged over the selected days that have clear skies at 12:00-13:00 local time for the wheat and corn growth stages at the Yucheng and Yingke sites.

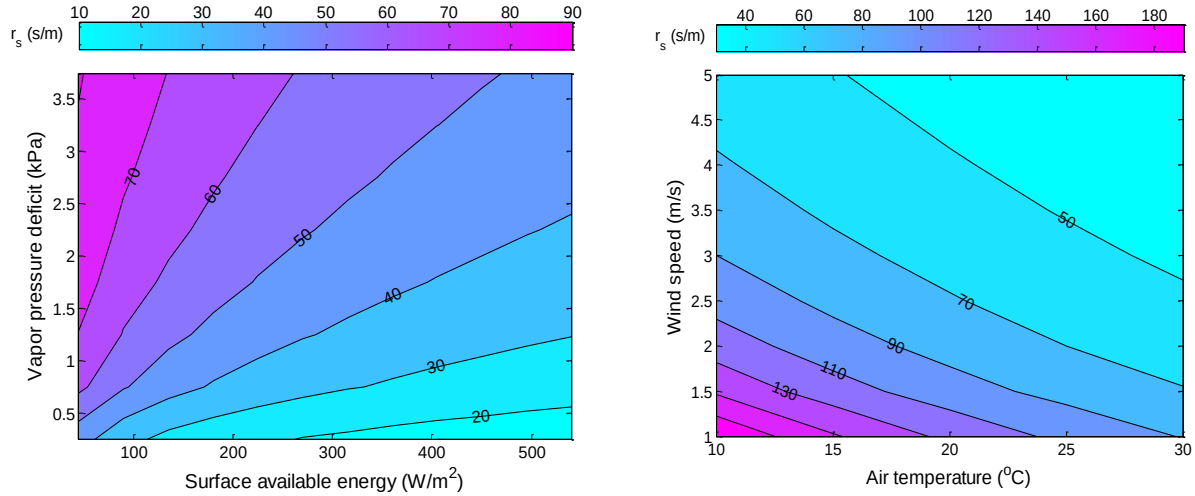


**Figure** 3. (**a**) Contour of Todorovic's variable surface resistance ($r_s$) with the variations of surface available energy and vapor pressure deficit, when air temperature is at 30 $^{o}$C and wind speed equals 3.0 m/s. (**b**) Contour of the $r_s$ with the variations of air temperature and wind speed, when surface available energy is at 450 W/m$^2$ and vapor pressure deficit equals 3.0 kPa.

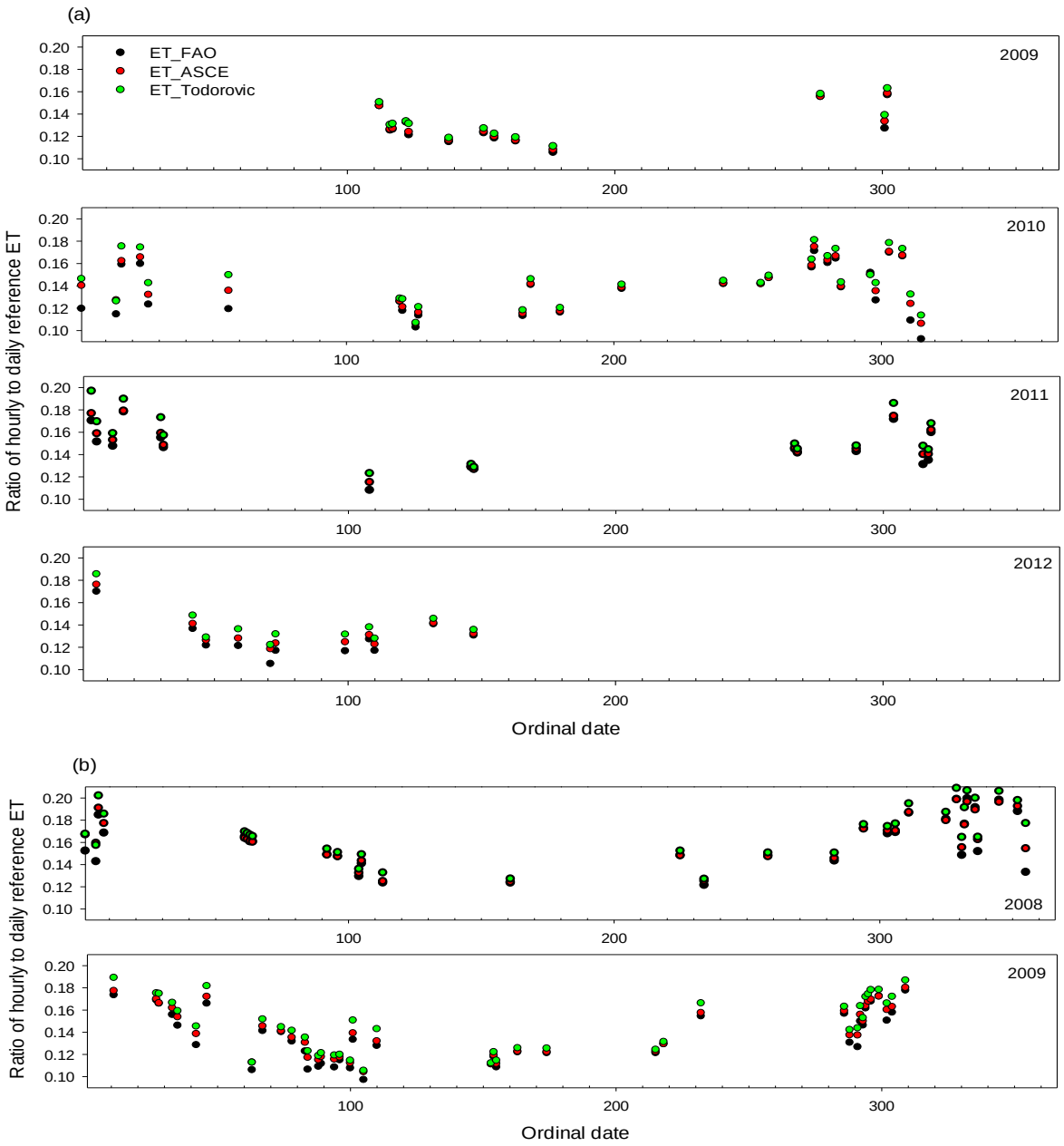


**Figure** 4. Temporal variation of the ratios of 12:00-13:00 local time hourly to daily latent heat flux estimated from the FAO-PM, the ASCE-PM, and the full-form PM equations over the selected days at (a) Yucheng site from year 2009 to 2012 and (b) Yingke site from year 2008 to 2009.

Using fixed and variable surface resistances results in different daytime half-hourly reference ET estimates and, consequently, influences the ratio of the reference instantaneous ET to the daily ET. Using the noon data as an example, Figure 4a-b illustrates how the ratios of the hourly to daily reference ETs ($ET_{r,h}/ET_{r,d}$) estimated from the FAO-PM, ASCE-PM, and full-form PM equations vary seasonally over the selected 68 days from April 2009 to June 2012 at the Yucheng site and over the selected 73 days from January 2008 to November 2009 at the Yingke site.

Overall, the $ET_{r,h}/ET_{r,d}$ computed at 12:00-13:00 local time from the three PM equations showed similar seasonal patterns and magnitudes at both sites; higher values occur in the winter and lower values occur in the summer, which reflects the temporal variations in the vapor pressure deficit, the surface available energy, and the disparate percentage of noon-time ET in the daily ET in a yearly cycle. In most cases, the $ET_{r,h}/ET_{r,d}$ ratio varied between ~0.1 and ~0.2 at both sites and was higher at the arid Yingke site than at the sub-humid Yucheng site. The $ET_{r,h}/ET_{r,d}$ using the full-form PM equation was generally higher than that using the ASCE-PM equation. Both were higher than that using the FAO-PM equation.

The discrepancy between the $ET_{r,h}/ET_{r,d}$ ratios estimated using the variable and fixed surface resistances was larger when the ET was small and smaller when the ET was large, which indicates that using these three surface resistances and PM equations in the constant $EF_r$ method would yield a larger relative difference in the upscaled daily ET in the winter than that in the summer. However, at both sites, the discrepancy between the $ET_{r,h}/ET_{r,d}$ ratios in the wheat growth stage with short grass as the reference crop was not significantly different from that in the corn growth stage with tall alfalfa as the reference crop.

## 4.2 Evaluation using original flux tower measurements

For a given time period, the paired-t test was used to test the null hypothesis that the mean of one PM model-predicted daily ET equals the mean of another PM model-predicted daily ET against the alternative hypothesis that the two statistics are not equal. After further selecting the days that had two assumed time periods, the paired-t test was separately used for all three PM equations to test the null hypothesis that the mean of the model-predicted ET at one time equals that at another time against the alternative hypothesis that the two statistics are not equal. The level of significance chosen for all tests was 0.05 (95% confidence level).

Figure 5a-f compares the daily ET measured by the EC without an energy correction and that ($ET_{FAO\text{-}PM}$, $ET_{ASCE\text{-}PM}$, and $ET_{TOD\text{-}PM}$) upscaled from the constant $EF_r$ method, with the reference ET derived using the FAO-PM equation, the ASCE-PM equation, and the full-form PM equation at the Yucheng and Yingke sites. The corresponding statistical measures of the performance are illustrated in Figure 6a-c. (i) Using the three PM equations produced significantly different upscaled daily LEs at a given time from mid-morning to mid-afternoon, with an exception occurring at the Yingke site in the mid-morning between using the ASCE-PM equation and the full-form PM equation. (ii) At the Yucheng site, using the ASCE-PM equation and the full-form PM equation overall produced the best results from mid-morning to noon and in the mid-afternoon, respectively. Using the FAO-PM equation produced the worst results for all time intervals. At the Yingke site, using the FAO-PM equation and the full-form PM equation produced the best and the worst results, respectively, from mid-morning to noon whereas the opposite results were obtained in the mid-afternoon. (iii) Using all three PM equations tended to produce progressively larger upscaled daily LE from mid-morning to mid-afternoon. For a given time, $ET_{FAO\text{-}PM} > ET_{ASCE\text{-}PM} > ET_{TOD\text{-}PM}$. (iv) For all three PM equations, the daily LE upscaled in the mid-morning was not significantly different from that in the noon time, and the model performances were overall statistically better in the mid-morning and noon time than those in the mid-afternoon.

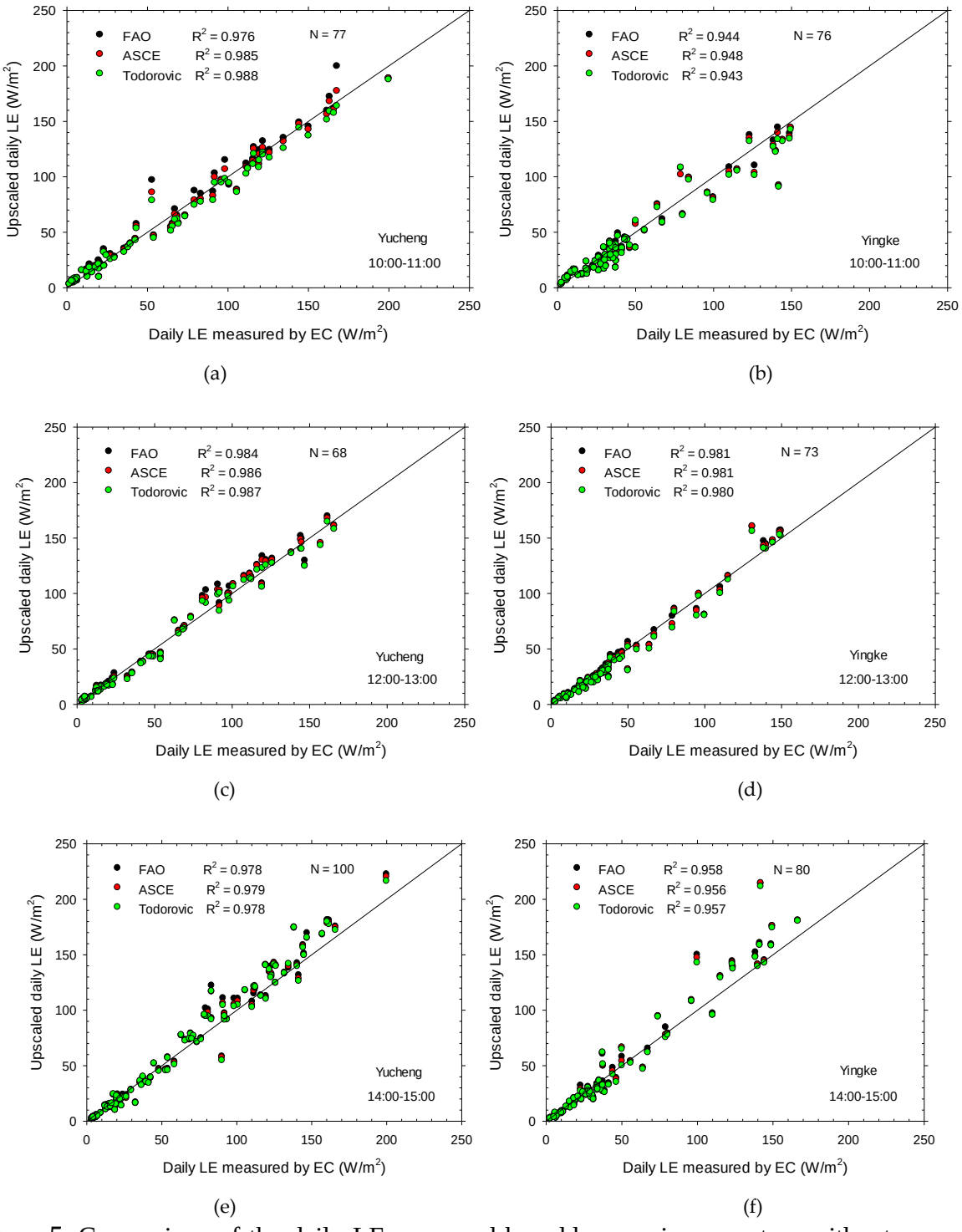


**Figure** 5. Comparison of the daily LE measured by eddy covariance system without an energy correction with that derived by the constant reference evaporative fraction method at three different local time periods in the daytime over selected clear skies. (**a**), (**c**), and (**e**) for the Yucheng site, (**b**), (**d**), and (**f**) for the Yingke site.

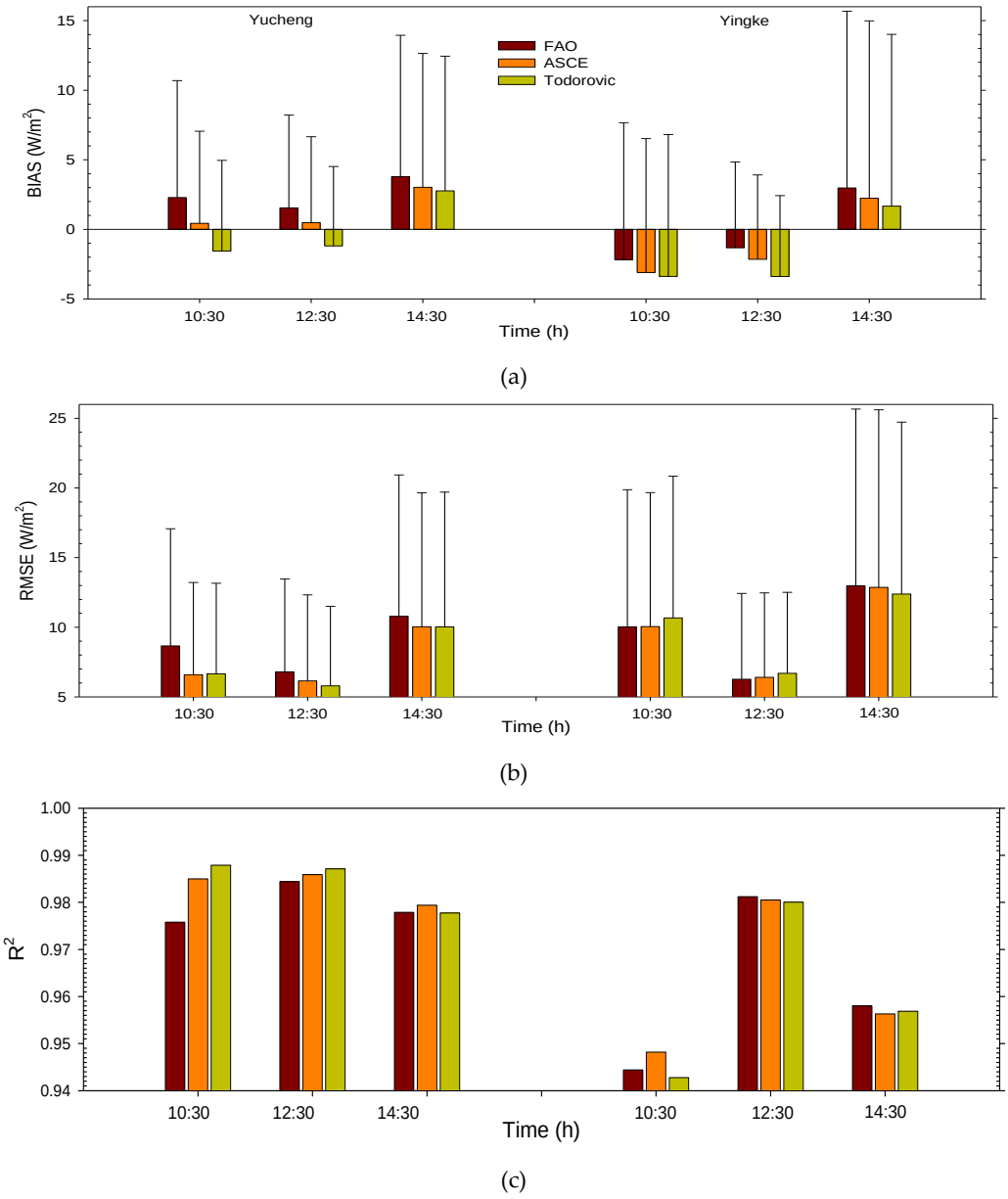


**Figure 6**. Statistical measures of the performance of constant reference evaporative fraction upscaling method in converting hourly ET estimated using the FAO-PM, the ASCE-PM, and the full-form PM equations at different clear sky time periods in the daytime to daily value over selected days (10:30 stands for 10:00-11:00 interval, similarly hereafter). The error bar represents one standard deviation of the difference between model-estimated and EC-measured daily ETs. For each of the panels, the left part is for the Yucheng site and the right part is for the Yingke site. The EC-measured LE was not corrected to close the energy imbalance. (**a**) BIAS, (**b**) root mean square error (RMSE), (**c**) coefficient of determination ($R^2$).

## 4.3 Evaluation using corrected flux tower measurements

The energy closure ratio, which is defined as the ratio of the sum of the half-hourly EC-measured H and LE to the surface available energy, for the quality-, completeness-, and relative

humidity-controlled days averaged 0.81 and 0.67 at the Yucheng and the Yingke sites, respectively. The paired-t test that was used in Section 4.2 was also applied in this section to evaluate the significance of the statistical results.

Figure 7a-c shows the statistical measures of the performance of the constant $EF_r$ upscaling method after using the BR correction method introduced in Section 3.3 to close the energy imbalance of the original EC measurements. At the Yucheng site, different from the results without the correction of surface energy imbalance, using the full-form PM equation and the FAO-PM equation produced the best and the worst results, respectively, from mid-morning to noon, whereas the opposite results were obtained in the mid-afternoon. At the Yingke site, using the three PM equations produced significantly different upscaled daily LEs at a given time from mid-morning to mid-afternoon with no exceptions. Using the FAO-PM equation and the full-form PM equation produced the best and worst results, respectively, from noon to mid-afternoon, whereas the opposite results were obtained in the mid-morning. Moreover, at both sites, using all three PM equations tended to produce progressively smaller upscaled daily LEs from mid-morning to mid-afternoon. For a given PM equation, the daily LE upscaled at one time was significantly different from that at another time from mid-morning to mid-afternoon (with an exception at the Yingke site for the full-form PM equation between noon time and mid-afternoon) and the best model performance tended to occur in the noon time.

Figure 8a-c shows the statistical measures of the performance of the constant $EF_r$ upscaling method when using the RE correction method to close the energy imbalance of the original EC measurements. At the Yucheng site, the results were completely the same as those obtained when the BR correction method was applied. At the Yingke site, the results were almost the same as those obtained using the BR correction method. The only difference was that the daily LE upscaled at one time for a given PM equation was significantly different from that at another time from mid-morning to mid-afternoon with no exceptions.

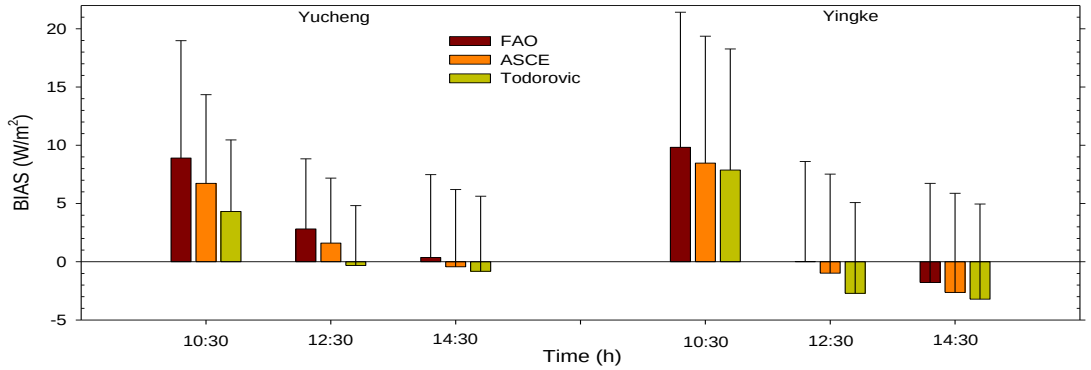


(a)

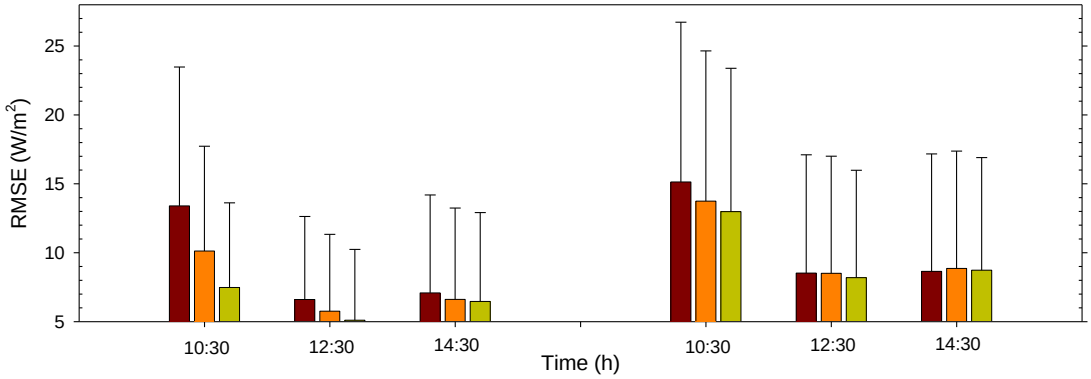


(b)

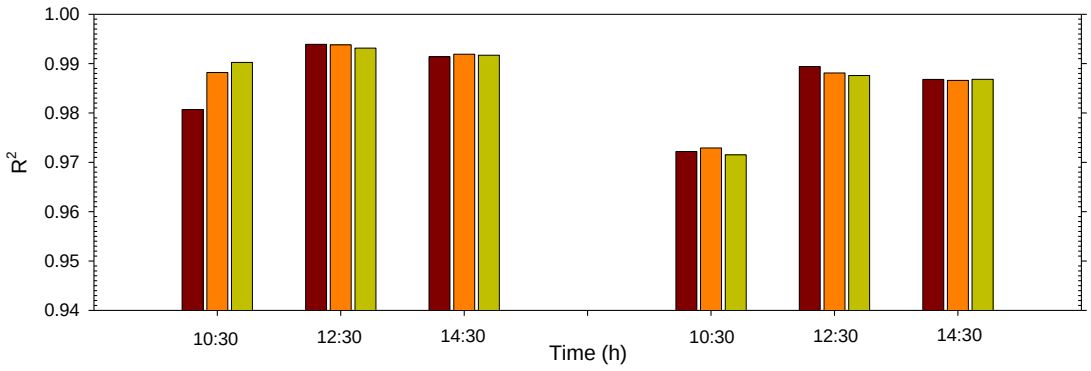


(c)

**Figure 7**. Comparison of  Same as Figure 6, but for the application of energy closure of the EC-measured LE using the Bowen ratio correction method.

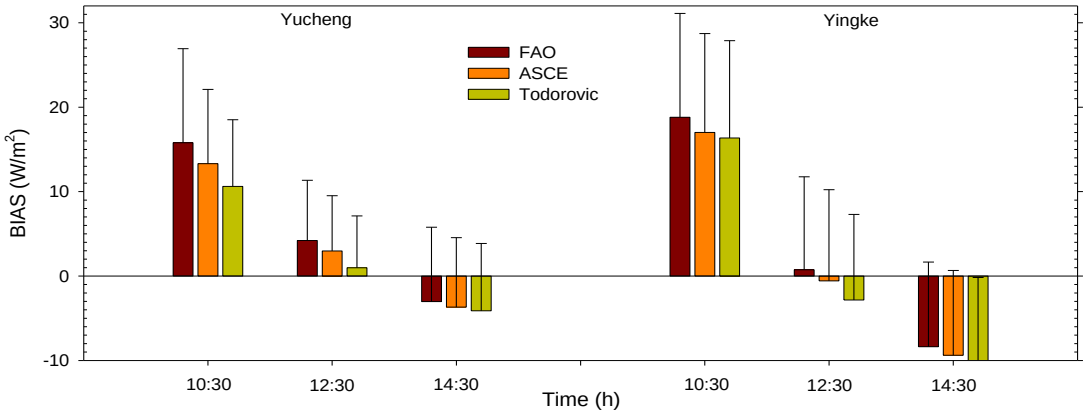


(a)

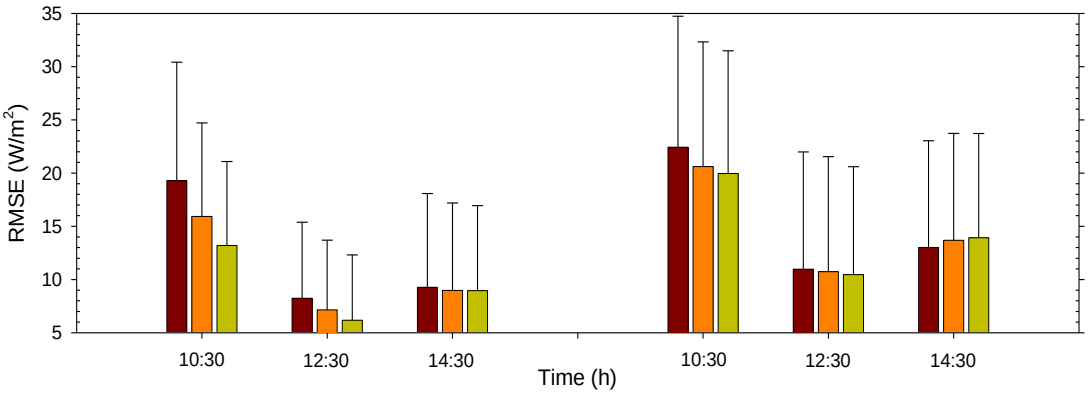


(b)

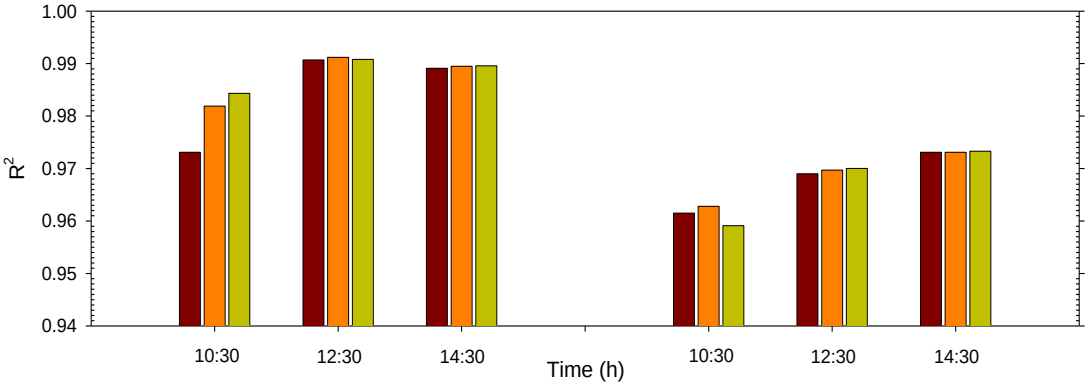


(c)

**Figure** 8. Same as Figure 6, but for the application of energy closure of the EC-measured LE using the residual energy correction method.

## 4.4 Discussion

The performance of the constant $EF_r$ upscaling method in practical applications depends on how close the instantaneous $EF_r$ at a given clear-sky satellite overpass time is to the daily average. When the instantaneous $EF_r$ is larger (or smaller) than the daily average, the upscaled daily LE will be overestimated (or underestimated). Using the constant $EF_r$ method to upscale the LE requires accurate estimates of the reference hourly and daily ET values.

Given the same magnitude of the decrease in the surface resistance for all of the hourly periods during the daytime, the relative increase in the hourly reference ET from mid-morning to mid-afternoon is generally larger than that in the early morning and late afternoon because the reference ET near midday accounts for the largest fraction of the daily average. Due to the combined effect of the reduced nighttime reference ET and the smaller increase in the early morning and late-afternoon reference ET values than the mid-morning to mid-afternoon reference ET values, the relative increase in the hourly reference ET from mid-morning to mid-afternoon will generally be greater than the relative increase in the daily average, which results in a larger $ET_{r,h}/ET_{r,d}$ and a smaller upscaled daily LE when using the ASCE-PM equation than when using the FAO-PM equation. In contrast, using the greater variable surface resistances derived from Todorovic's method than the fixed values adopted in the ASCE-PM equation produced smaller daytime reference ET estimates and, consequently, smaller daily reference ET estimates. Because the variable surface resistance has a concave shape during the daytime, the relative decrease in the hourly reference ET has a convex shape, and its absolute value is significantly smaller in the midday period than in the early morning and late afternoon. This most likely produces a larger $ET_{r,h}/ET_{r,d}$ in the full-form PM equation than that in the ASCE-PM equation and a smaller upscaled daily LE. The large standard deviation as shown in Figures 6-8 may indicate the instability of the $EF_r$ in a diurnal cycle under some circumstances over the wide range of atmospheric and soil moisture conditions at both sites (in other words, using the constant $EF_r$ upscaling method can create a large bias in the daily ET).

Progressively smaller upscaled daily ET values from mid-morning to mid-afternoon using the constant $EF_r$ method have also been found in previous studies [*Cammalleri et al.,* 2014; *Tang et al.,* 2013a]. When the upscaled daily ET values from the constant $EF_r$ method were compared to the EC measurements without an energy imbalance correction, the overestimation (positive bias) during the mid-morning and underestimation (negative bias) during the mid-afternoon in this study and our prior study [*Tang et al.,* 2013a] were not consistent with the results of *Cammalleri et al.* [2014], who found a stable underestimation in the upscaled daytime ET from mid-morning to mid-afternoon. Our finding that the noon time overall appeared to be the optimal time for instantaneous ET upscaling has also been revealed by other researchers [*Colaizzi et al.,* 2006; *Delogu et al.,* 2012; *Tang et al.,* 2013a; *Cammalleri et al.,* 2014]. Because the $ET_{r,h}/ET_{r,d}$ does not vary before and after the energy imbalance correction, how the model performance of a given PM equation changes with the energy closure at a given time entirely depends on the relative variation in the corrected hourly and daily EC-measured ET. This may also lead to a change in the same inter-model performances of the three PM equations. Site-to-site and time-to-time variations were found in this study in the performances of a given PM equation before and after the energy imbalance was closed, which agreed with *Cammalleri et al.* [2014] and *Tang et al.* [2013a], who found that the closure of EC measurements could have a significant effect on the choice of optimal upscaling technique. Because no studies have ever attempted to incorporate a variable daytime surface resistance in the upscaling of instantaneous ET data using the constant $EF_r$ method, our findings that are associated with the best upscaling technique and the optimal

upscaling time in the three PM equations in this study cannot be further corroborated by the work of other authors.

Unexpectedly, using variable surface resistances did not produce a much closer upscaled daily ET to using a fixed surface resistance as adopted in the ASCE-PM equation at the sub-humid Yucheng site than at the arid Yingke site. This may be because the reference ET estimate is controlled not by the absolute value of the surface resistance but primarily by the ratio of the surface to aerodynamic resistances; both resistances generally have similar diurnal patterns. Underestimated daily LE values upscaled from the constant $EF_r$ method at 12:00-13:00 local time using Todorovic's variable surface resistance in the reference ET estimates at the arid site in this study are also found in the work of *Liu et al.* [2012] when the BR correction method is applied to close the energy imbalance of the EC measurements. Both studies produced relative root mean square errors (RMSEs, ratio of the RMSE to the observed mean) with similar magnitudes. However, the constant $EF_r$ method using Todorovic's variable surface resistance performs better at the humid Yucheng site than at the arid Yingke site, with lower (relative) absolute BIAS and RMSE values but a higher coefficient of determination ($R^2$). This may be explained by the explanation by *Allen et al.* [2006] that the climatic resistance model of Todorovic works reasonably well for rain-fed agriculture but can fail in irrigated areas in semi-arid and arid climates. Based on studies by European and American researchers, *Allen et al.* [2006] recommended using fixed surface resistance values of 50 s/m for daytime and 200 s/m for nighttime for the reference ET estimates. Nevertheless, several authors have demonstrated that using variable surface resistances is preferential to using a fixed surface resistance of 70 m/s for daytime reference ET estimates, even at semi-arid sites [*Todorovic,* 1999; *Lecina et al.,* 2003; *Perez et al.,* 2006]. Moreover, using variable surface resistances in this study was indeed able to produce better daily ET estimates in the constant $EF_r$ upscaling method in the mid-afternoon compared to using fixed surface resistances at both the Yucheng and Yingke sites when the energy imbalance of the EC measurements was not closed.

The low energy closure ratio (0.67 at the Yingke site) or the surface energy imbalance can be caused by a number of other factors [*Wilson et al.,* 2002; *Foken,* 2008; *Stoy et al.,* 2013], among which include the measurement errors of surface energy components, the mismatch of source areas between surface flux components, the uncorrection of heat storage for *G*, the neglect of the heat storage in the canopy, the neglect of photosynthetic and advective energy, and the dispersive fluxes not sampled by the EC system. The reasons for the closure errors in the EC measurements are difficult to realistically identify because so many factors can influence the energy imbalance. These various influencing factors and the applied correction methods can have an impact on the EC-measured ET and the validation results of upscaled daily ET. The error in the validation of upscaled daily ET is therefore difficult to attribute to a certain factor (e.g., poor *G* representation) or a correction method. Nevertheless, knowledge of the model performances under given conditions at the Yucheng and Yingke sites is still valuable.

The limitation in using the constant $EF_r$ upscaling method primarily lies in its requirement of metrological measurements (solar radiation, air temperature, vapor pressure deficit, wind speed) as inputs. However, a great advantage of using this method towards other simpler scaling techniques (e.g., using at-surface solar radiation as the reference variable, as in *Cammalleri et al.* [2014] and using surface net radiation as the reference variable, as in *Nagler et al.* [2009]) is that it can incorporate the effect of advective energy and time-dependent environmental variables on the ET in a diurnal cycle. Moreover, deriving a variable resistance does not require inputs any more than estimating the reference ET from the Penman-Monteith equation when the constant

$EF_r$ upscaling method is applied. Using variable surface resistance could potentially improve the reference ET estimates and thus the ET upscaling in the constant EFr method [*Liu et al.,* 2012; *Pereira et al.,* 1999; *Rana and Katerji,* 2000; *Lecina et al.,* 2013; *Perez et al.,* 2006].

## 5 Summary and conclusions

In the upscaling of instantaneous ET, both the constant $EF_r$ method and the constant global solar radiation ratio method outperform the constant evaporative fraction method, the constant extraterrestrial solar radiation ratio method, and the sinusoidal function method, though there is no agreement on which of the former two methods performs better [*Xu et al.,* 2015; *Tang et al.,* 2013; *Cammalleri et al.,* 2014]. To investigate whether the use of a variable surface resistance in the reference ET estimation from the PM equation, as proposed by *Todorovic* [1999], can improve the daily upscaled ET on clear-sky days from the constant $EF_r$ method, half-hourly near-surface meteorological variables and EC-measured LE values were collected as the model inputs and validation data, respectively, at two sites with contrasting climatic conditions, namely, the sub-humid Yucheng station in northern China and the arid Yingke site in northwestern China. The use of Todorovic's variable surface resistance in this study does not require a priori calibration.

The results before the energy imbalance in the EC measurements was closed are summarized as follows:

i) In the mid-afternoon, using variable surface resistance in the full-form PM equation at both sites produced the best ET upscaling results, and using fixed resistance in the FAO-PM equation produced the worst results.

ii) In the mid-morning to noon, using fixed resistance in the ASCE-PM equation at the Yucheng site produced the best results, and using the FAO-PM equation produced the worst results. At the Yingke site, using the FAO-PM equation and the full-form PM equation produced the best and worst results, respectively.

iii) For all three PM equations, the daily LE upscaled in the mid-morning was not significantly different from that in the noon time, and the model performances were overall statistically better in the mid-morning and noon time than in the afternoon.

iv) At both sites, using all three PM equations tended to produce progressively larger upscaled daily LEs from mid-morning to mid-afternoon. For a given time, $ET_{FAO\text{-}PM} > ET_{ASCE\text{-}PM} > ET_{TOD\text{-}PM}$.

After the energy imbalance was closed using the BR and RE correction methods, some changes were found in the results as follows:

i) In the mid-morning, using the full-form PM equation at both sites produced the best results, and using fixed resistance in the FAO-PM equation produced the worst results.

ii) In the mid-afternoon, using the FAO-PM equation and the full-form PM equation at the Yucheng site produced the best and the worst results, respectively. The opposite results were obtained at the Yingke site.

iii) In the noon time, using the full-form PM equation at the Yucheng site produced the best results, and using the FAO-PM equation produced the worst results. The opposite results were obtained at the Yingke site.

iv) For a given PM equation, the daily LE upscaled at one time was significantly different from that at another time from mid-morning to mid-afternoon, and the best model performance tended to occur in the noon time.

v) At both sites, using all three PM equations tended to produce progressively smaller upscaled daily LEs from mid-morning to mid-afternoon.

In summary, using the three PM equations produced significantly different upscaled daily ETs ($ET_{FAO\text{-}PM} > ET_{ASCE\text{-}PM} > ET_{TOD\text{-}PM}$) at a given time from mid-morning to mid-afternoon. Using all three PM equations overall produced the best results at noon at both sites regardless of whether the energy imbalance was closed. When the EC measurements were not corrected for energy imbalance, using variable surface resistance in the full-form PM equation could improve the ET upscaling in the mid-afternoon, but worse results may occur in the mid-morning to noon. Site-to-site and time-to-time variations were found in the performances of a given PM equation before and after the energy imbalance was closed. At a given site, using the BR correction method yields the same inter-model performances for the three PM equations as using the RE correction method. It has to be mentioned that when detailed meteorological measurements are not available at the ground station, to temporally upscale the remote sensing instantaneous ET in a practical application using the constant $EF_r$ method, regional reference ET can be estimated with reanalysis data from numerical weather prediction models and global climate models (Tian and Martinez 2012; Ishak et al. 2010). When soil heat flux measurement is not available, to close the energy imbalance of EC measurements, semi-empirical relationships as proposed by kustas and Daughtry (1990), Bastiaanssen et al. (1998), and Su (2002) can be applied to derive a spatially representative soil heat flux from surface net radiation measurement and remote sensing vegetation index. Note that although the evaluation in this study is only conducted at two sites, it is instructive and can be conclusive to a great extent because these two sites are characterized by contrasting climatic conditions and data involved cover a wide range of soil moisture and vegetation cover conditions. To make a general conclusion, more extensive assessments and validations are required over a wider range of climate, soil moisture, and plant functional type conditions.

## Acknowledgments and Data

The staff members at the Yucheng site are acknowledged for their hard-work on the setup and maintenance of the ground-based instruments and data collection. Associate Professor Yuanyuan Jia and Professor Chuanrong Li in the Academy of Opto-Electronics, Chinese Academy of Sciences, are thanked for their cooperation in providing the surface measurements. EC data at the Yingke site used in this study are downloaded from "Environmental & Ecological Science Data Center for West China, National Natural Science Foundation of China, http://westdc.westgis.ac.cn". This work was partly supported by the National Natural Science Foundation of China under Grant 41571351 and 41571367, and in part by the International Science and Technology Cooperation Program of China under Grant 2014DFE10220.

## References

Allen, R. G., L. S. Pereira, D. Raes, and M. Smith (1998), Crop evapotranspiration-Guidelines for computing crop water requirements, FAO Technical Paper 56, Food and Agricultural Organization of the United Nations, Rome, 300(9), D05109.

Allen, R. G., W. O. Pruitt, J. L. Wright, T. A. Howell, F. Ventura, R. Snyder, D. Itenfisu, P. Steduto, J. Berengena, J. Yrisarry, M. Smith, L. Pereira, D. Raes, A. Perrier, I. Alves, I. Walter, and R. Elliott (2006), A recommendation on standardized surface resistance for

hourly calculation of reference ETo by the FAO56 Penman-Monteith method, *Agr. Water Manage.*, *81*(1), 1-22, doi:10.1016/j.agwat.2005.03.007.

Allen, R. G., M. Tasumi, and R. Trezza (2007), Satellite-based energy balance for mapping evapotranspiration with internalized calibration (METRIC)-model, *J Irrig. Drain. E.*, *133*(4), 380–394, doi: 10.1061/(ASCE)0733-9437(2007)133:4(380).

Alves, I., and L. S. Pereira (2000), Modelling surface resistance from climatic variables?, *Agr. Water Manage.*, *42*(3), 371-385, doi: 10.1016/S0378-3774(99)00041-4.

ASCE-EWRI. (2005), The ASCE Standardized Reference Evapotranspiration Equation. Technical Committee report to the Environmental and Water Resources Institute of the American Society of Civil Engineers from the Task Committee on Standardization of Reference Evapotranspiration, ASCE-EWRI, 1801 Alexander Bell Drive, Reston, VA 20191-4400, 173 pp, doi:10.1061/40499(2000)126.

Baldocchi, D., E. Falge, L. Gu, R. Olson, D. Hollinger, S. Running, P. Anthoni, C. Bernhofer, K. Davis, R. Evans, J. Fuentes, A. Goldstein, G. Katul, B. Law, X. Lee, Y. Malhi, T. Meyers, W. Munger, W. Oechel, K. Paw, K. Pilegaard, H. Schmid, R. Valentini, S. Verma, T. Vesala, K. Wilson, and S. Wofsy (2001), FLUXNET: A new tool to study the temporal and spatial variability of ecosystem-scale carbon dioxide, water vapor, and energy flux densities, *B. AM. Meteorol. Soc.*, *11*, 2415-2434, doi:10.1175/1520-0477(2001)082<2415:FANTTS>2.3.CO.

Bastiaanssen, W. G. M., M. Menenti, R. A. Feddes, and A. A. M. Holtslag (1998), A remote sensing surface energy balance algorithm for land (SEBAL). 1. Formulation, *J. Hydrol*., *212*, 198-212, doi:10.1016/S0022-1694(98)00254-6.

Brutsaert, W., and M. Sugita (1992), Application of self-preservation in the diurnal evolution of the surface energy budget to determine daily evaporation, *J. Geophys. Res.*, *97*, 18377-18382, doi:10.1029/92JD00255.

Burba, G., and D. Anderson (2010), A brief practical guide to eddy covariance flux measurements: principles and workflow examples for scientific and industrial applications, LI-COR Biosciences, Lincoln, Nebraska, USA, 212 pp, doi:10.13140/RG.2.1.1626.4161.

Cammalleri, C., M. C. Anderson, and W. P. Kustas (2014), Upscaling of evapotranspiration fluxes from instantaneous to daytime scales for thermal remote sensing applications, *Hydrol. Earth Syst. Sc.*, *18*, 1885-1894, doi:10.5194/hess-18-1885-2014.

Chávez, J. L., C. M. Neale, J. H. Prueger, and W. P. Kustas (2008), Daily evapotranspiration estimates from extrapolating instantaneous airborne remote sensing ET values, *Irrigation. Sc.*, *27*, 67-81, doi:10.1007/s00271-008-0122-3.

Colaizzi, P. D., S. R. Evett, T. A. Howell, and J. A. Tolk (2006), Comparison of five models to scale daily evapotranspiration from one-time-of-day measurements, *T. ASAE.*, *49*, 1409-1417, doi:10.13031/2013.22056.

Delogu, E., G. Boulet, A. Olioso, B. Coudert, j. Chirouze, E. Ceschi, B. Le Dantec, O. Marloie, G. Chehbouni, and J.-P. Lagouarde (2012), Reconstruction of temporal variations of evapotranspiration using instantaneous estimates at the time of satellite overpass, *Hydrol. Earth Syst. Sc.*, *16*, 2995-3010, doi:10.5194/hess-16-2995-2012.

714 Foken, T. (2008). The energy balance closure problem: An overview, *Ecol. Appl.*, *18*, 1351-
715 1367, doi:10.1890/06-0922.1.

716 Jackson, R. D., J. L. Hatfield, R. J. Reginato, S. B. Idso, and P. Pinter (1983), Estimation of daily
717 evapotranspiration from one time of day measurements, *Agr. Water Manage.*, *7*, 351-362,
718 doi:10.1016/0378-3774(83)90095-1.

719 Ishak, A. M., M. Bray, R. Remesan, and D. Han (2010), Estimating reference evapotranspiration
720 using numerical weather modelling, *Hydrol. Process.*, *24*(24), 3490–3509,
721 doi:10.1002/hyp.7770.

722 Jia, L., G. Xi, S. Liu, C. Huang, Y. Yan, and G. Liu (2007), Regional estimation of daily to
723 annual regional evapotranspiration with MODIS data in the Yellow River Delta wetland,
724 *Hydrol. Earth Syst. Sci.*, *13*, 1775–1787, doi:10.5194/hessd-6-2301-2009.

725 Kalma, J. D., T. R. McVicar, and M. F. McCabe (2008), Estimating land surface evaporation: a
726 review of methods using remotely sensed surface temperature data, *Surv. Geophys.*, *29*,
727 421−469, doi:10.1007/s10712-008-9037-z.

728 Katerji, N., A. Perrier, D. Renard, and A. K. O. Aissa (1983), Modélisation de
729 l'évapotranspiration réelle ETR d'une parcelle de luzerne: rôle d'un coefficient cultural,
730 *Agronomie.*, *3*(6), 513-521, doi:10.1051/agro:19830603.

731 Kustas, W. P., and C. S. T. Daughtry (1990), Estimation of the soil heat flux/net radiation ratio
732 from spectral data, *Agr. Forest Meteor.*, *49*, 205−223, doi:10.1016/0168-1923(90)90033-
733 3.

734 Lecina, S., A. Martınez-Cob, P. J. Pérez, F. J. Villalobos, and J. J. Baselga (2003), Fixed versus
735 variable bulk canopy resistance for reference evapotranspiration estimation using the
736 Penman-Monteith equation under semiarid conditions, *Agr. Water Manage.*, *60*(3), 181-
737 198, doi:10.1016/S0378-3774(02)00174-9.

738 Li, Z. -L., R. L. Tang, Z. Wan, Y. Bi, C. Zhou, B. Tang, G. Yan, and X. Zhang (2009), A Review
739 of current methodologies for regional evapotranspiration estimation from remotely
740 sensed data, *Sensors*, *9*, 3801−3853, doi:10.3390/s90503801.

741 Li, Z. -L., B. H. Tang, H. Wu, H. Ren, G. Yan, Z. Wan, I. F. Trigo, and J. A. Sobrino (2013a),
742 Satellite-derived land surface temperature: Current status and perspectives, *Remote Sens.*
743 *Environ.*, *131*, 14-37, doi:10.1016/j.rse.2012.12.008.

744 Li, Z. -L., H. Wu, N. Wang, S. Qiu, J. A. Sobrino, Z. Wan, B. Tang, and G. Yan (2013b), Land
745 surface emissivity retrieval from satellite data, *Int. J. Remote Sens.*, *34*(9-10), 3084-3127,
746 doi:10.1080/01431161.2012.716540.

747 Liu, G., M. Hafeez, Y. Liu, D. Xu, and C. Vote (2012), A novel method to convert daytime
748 evapotranspiration into daily evapotranspiration based on variable canopy resistance, *J.*
749 *Hydrol.*, *414*, 278-283, 10.1016/j.jhydrol.2011.10.042.

750 Liu, S. M., Z. W. Xu, W. Z. Wang, Z. Z. Jia, M. J. Zhu, J. Bai, and J. M. Wang (2011), A
751 comparison of eddy-covariance and large aperture scintillometer measurements with
752 respect to the energy balance closure problem, *Hydrol. Earth Syst. Sc.*, *15*(4), 1291-1306,
753 doi:10.5194/hess-15-1291-2011.

754 Nagler, P. L., K. Morino, R. S. Murray, J. Osterberg, and E. P. Glenn (2009), An empirical
755 algorithm for estimating agricultural and riparian evapotranspiration using MODIS
756 enhanced vegetation index and ground measurements of ET. I. Description of method,
757 *Remote Sens.*, *1*(4), 1273-1297, doi:10.3390/rs1041125.

758 Pereira, L. S., A. Perrier, R. G. Allen, and I. Alves (1999), Evapotranspiration: concepts and
759 future trends, *J. Irrig. Drain. E.*, *125*(2), 45-51, doi:10.1061/(ASCE)0733-
760 9437(1999)125:2(45).

761 Perez, P. J., S. Lecina, F. Castellvi, A. Martínez−Cob, and F. J. Villalobos (2006), A simple
762 parameterization of bulk canopy resistance from climatic variables for estimating hourly
763 evapotranspiration, *Hydrol. Process.*, *20*(3), 515-532, doi:10.1002/hyp.5919.

764 Rana, G., and N. Katerji (2000), Measurement and estimation of actual evapotranspiration in the
765 field under Mediterranean climate: a review, *Eur. J. Agron.*, *13*(2), 125-153,
766 doi:10.1016/S1161-0301(00)00070-8.

767 Ryu, Y., D. D. Baldocchi, T. A. Black, M. Detto, B. E. Law, R. Leuning, A. Miyata, M.
768 Reichstein, R. Vargas, C. Ammann, J. Beringer, L. Flanagan, L. Gu, L. Hutley, J. Kim,
769 H. McCaughey, E. Moors, S. Rambal, and T. Vesala (2012), On the temporal upscaling
770 of evapotranspiration from instantaneous remote sensing measurements to 8-day mean
771 daily-sums, *Agr. Forest Meteor.*, *152*, 212-222, doi:10.1016/j.agrformet.2011.09.010.

772 Shuttleworth, W. J., R. J. Gurney, A. Y. Hsu, and J. P. Ormsby (1989), FIFE: the variation in
773 energy partition at surface flux sites, *Int. Assoc. Hydrol. Sc.Publ.*, *186*, 67–74.

774 Stoy, P. C., M. Mauder, T. Foken, B. Marcolla, E. Boegh, A. Ibrom, A. Arain, A. Arneth, M.
775 Aurela, B. Bernhofer, A. Cescatti, E. Kellwik, P. Duce, D. Gianelle, E. Gorsel, G. Kiely,
776 A. Knohl, H. Margolis, H. McCaughey, L. Merbold, L. Montagnani, D. Papale, M.
777 Reichstein, M. Saunders, P. Serrana-Ortiz, M. Sottocornola, D. Spano, F. Vaccari, and A.
778 Varlagin (2013), A data-driven analysis of energy balance closure across FLUXNET
779 research sites: The role of landscape scale heterogeneity, *Agr. Forest Meteor.*, *171*, 137-
780 152, doi:10.1016/j.agrformet.2012.11.004.

781 Su, Z. (2002), The surface energy balance system (SEBS) for estimation of turbulent heat fluxes,
782 *Hydrol. Earth Syst. Sc.*, *6*, 85−99, doi:10.5194/hess-6-85-2002.

783 Sugita, M., and W. Brutsaert (1991), Daily evaporation over a region from lower boundary layer
784 profiles measured with radiosondes, *Water Resour. Res.*, *27*, 747–752,
785 doi:10.1029/90WR02706.

786 Sun, Z., Q. Wang, B. Matsushita, T. Fukushima, Z. Ouyang, and M. Watanabe (2009),
787 Development of a simple remote sensing evapotranspiration model (Sim-ReSET):
788 algorithm and model test, *J. Hydrol.*, *376*(3), 476-485, doi:10.1016/j.jhydrol.2009.07.054.

789 Tang, R. L., Z. -L. Li, Y. Jia, C. Li, X. Sun, W. P. Kustas, and M. C. Anderson (2011a), An
790 intercomparison of three remote sensing-based energy balance models using Large
791 Aperture Scintillometer measurements over a wheat-corn production region, *Remote*
792 *Sens. Environ.*, *115*, 3187–3202, doi:10.1016/j.rse.2011.07.004.

Tang, R. L., Z. -L. Li, and K. S. Chen (2011b), Validating MODIS−derived land surface evapotranspiration with in situ measurements at two AmeriFlux sites in a semiarid region, *J. Geophys. Res-Atmo.*, (1984-2012), *116*(D4), doi:10.1029/2010JD014543.

Tang, R. L., Z. -L. Li, and X. Sun (2013a), Temporal upscaling of instantaneous evapotranspiration: An intercomparison of four methods using eddy covariance measurements and MODIS data, *Remote Sens. Environ.*, *138*, 102-118, doi:10.1016/j.rse.2013.07.001.

Tang, R. L., Z. -L. Li, and B. Tang (2010), An application of the Ts-VI triangle method with enhanced edges determination for evapotranspiration estimation from MODIS data in arid and semi-arid regions: Implementation and validation, *Remote Sens. Environ.*, *114*(3), 540-551, doi:10.1016/j.rse.2013.07.001.

Tang, R. L., Z. -L. Li, K. S. Chen, Y. Zhu, and W. Liu (2012), Verification of land surface evapotranspiration estimation from remote sensing spatial contextual information, *Hydrol. Process.*, *26*(15), 2283-2293, doi:10.1002/hyp.8341.

Tang, R. L., Z. -L. Li, Y. Jia, C. Li, K. S. Chen, X. Sun, and J. Lou (2013b), Evaluating one-and two-source energy balance models in estimating surface evapotranspiration from Landsat-derived surface temperature and field measurements, *Int. J. Remote Sens.*, *34*(9-10), 3299-3313, doi:10.1080/01431161.2012.716529.

Tian, D., and C. J. Martinez (2012), Forecasting reference evapotranspiration using retrospective forecast analogs in the southeastern United States, *J. Hydrometeorol.*, *13*(6), 1874–1892, doi:10.1175/JHM-D-12-037.1.

Todorovic, M. (1999), Single-layer evapotranspiration model with variable canopy resistance, *J. Irrig. Drain. E.*, *125*(5), 235-245, doi:10.1061/(ASCE)0733-9437(1999)125:5(235).

Trezza, R. (2002), Evapotranspiration using a satellite-based surface energy balance with standardized ground control, Ph.D. dissertation, USU, Logan, UT, 339 pp.

Twine, T. E., W. P. Kustas, J. M. Norman, D. R. Cook, P. R. Houser, T. P. Meyers, J. H. Prueger, P. J. Starks, and M. L. Wesely (2000), Correcting eddy-covariance flux underestimates over a grassland, *Agr. Forest Meteor.*, *103*, 279-300, doi:10.1016/S0168-1923(00)00123-4.

Van Niel, T. G., T. R. McVicar, M. L. Roderick, A. I. Van Dijk, J. Beringer, L. Hutley, and E. Van Gorsel (2012), Upscaling latent heat flux for thermal remote sensing studies: comparison of alternative approaches and correction of bias, *J. Hydrol.*, *468-469*, 35-46, doi:10.1016/j.jhydrol.2012.08.005.

Webb, E. K., G. I. Pearman, and R. Leuning (1980), Correction of flux measurements for density effects due to heat and water vapour transfer, *Q. J. Roy. Meteor. Soc.*, *106*(447), 85-100, doi:10.1002/qj.49710644707.

Wilson, K., A. Goldstein, E. Falge, M. Aubinet, D. Baldocchi, P. Berbigier, C. Bernhofer, R. Ceulemans, H. Dolman, C. Field, A. Grelle, A. Lbrom, B. Law, A. Kowalski, T. Meyers, J. Moncrieff, R. Monson, W. Oechel, J. Tenhunen, R. Valentini, and S. Verma (2002), Energy balance closure at FLUXNET sites, *Agr. Forest Meteor.*, *113*, 223-243, doi:10.1016/S0168-1923(02)00109-0.

Xu, T., S. Liu, L. Xu, Y. Chen, Z. Jia, Z. Xu, and J. Nielson (2015), Temporal upscaling and reconstruction of thermal remotely sensed instantaneous evapotranspiration, *Remote Sens.*, 7, 3400-3425, doi:10.3390/rs70303400.

Yu, G. R., X. F. Wen, X. M. Sun, B. D. Tanner, X. Lee, and J. Y. Chen (2006), Overview of ChinaFLUX and evaluation of its eddy covariance measurement, *Agr. Forest Meteor.*, *137*, 125–137, doi:10.1016/j.agrformet.2006.02.011.

Yu, Q., G. N. Flerchinger, S. Xu, J. Kozak, L. Ma, and L. Ahuja (2007), Energy balance simulation of a wheat canopy using the RZ-SHAW (RZWQM-SHAW) model, *Trans. ASABE, 50*(5), 1507-1516, doi: 10.13031/2013.23948.